CHEMISTRY OF MATERIALS

ARTICLE

pubs.acs.org/cm

$Li(H_2O)_{2-x}[Zr_2(PO_4)_3]$: A Li-Filled Langbeinite Variant ($x = 0$) as a Precursor for a Metastable Dehydrated Phase ($x = 2$)

Shuang Chen,[†] Stefan Hoffmann,[†] Katja Weichert,[‡] Joachim Maier,[‡] Yurii Prots,[†] Jing-Tai Zhao,[§] and Rüdiger Kniep*[,†]

[†]Max Planck Institute for Chemical Physics of Solids, Nöthnitzer Str. 40, 01187 Dresden, Germany

[‡]Max Planck Institute for Solid State Research, D-70569 Stuttgart, Germany

[§]State Key Laboratory of High Performance Ceramics and Superfine Microstructure, Shanghai Institute of Ceramics, Chinese Academy of Sciences, Shanghai 200050, People's Republic of China

Supporting Information

ABSTRACT: $Li(H_2O)_{2-x}[Zr_2(PO_4)_3]$ ($x = 0$) was synthesized under mild hydrothermal conditions. The crystal structure (single-crystal X-ray diffraction (XRD) data: cubic, space group $P2_13$ (No. 198), $a = 10.2417(1)$ Å, $V = 1074.28(2)$ Å^3, $Z = 4$) contains a langbeinite-framework consisting of ZrO_6 octahedra and PO_4 tetrahedra sharing common corners. H_2O molecules (crystal water) occupy the large cages extending along the 3-fold axes, thereby completing the langbeinite-type structural arrangement: $\{(H_2O)_2[Zr_2(PO_4)_3]\}^-$ vs $K_2[Mg_2(SO_4)_3]$. The filled langbeinite variant is completed by additional Li^+ ions taking positions between two neighboring water molecules and via the formation of linear arrangements $H_2O\cdots Li^+\cdots OH_2$. The thermochemical properties of $Li(H_2O)_{2-x}[Zr_2(PO_4)_3]$ ($0 \le x \le 2$) were studied by thermogravimetry−differential thermal analysis (TG-DTA), as well as by isothermal annealing combined with powder XRD investigations. Above 200 °C, the crystal water of the cubic hydrate is irreversibly released and the dehydrated phase keeps the cubic host structure. The dehydrated phase is metastable and transforms exothermally to a stable phase (probably the α-phase; NASICON-type structure) during heating (dynamic, 10 °C/min) at ∼970 °C. Depending on the maximum temperatures chosen for long-time annealing procedures (1180 and 800 °C, respectively) the α and β high-temperature phases (rhombohedral and orthorhombic, respectively) are formed, which undergo reversible phase transitions to the α′ (∼60 °C) and the β′ low-temperature phases (∼300 °C), respectively. Although the dehydrated cubic phase can be expected to show a high Li-ion conductivity, the metastable character of this phase will prevent any application without further stabilization of the crystal structure.

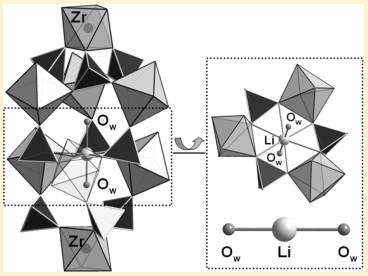

KEYWORDS: single crystal growth, langbeinite, structural characterization, thermal analysis

1. INTRODUCTION

Langbeinites, which are named after the naturally occurring mineral $K_2Mg_2(SO_4)_3$ (space group $P2_13$),[1] form a large group of compounds with the general chemical formula $A_xM_2(XO_4)_3$ (A = K^+, Rb^+, Cs^+, Tl^+, NH_4^+, etc.; M = Zn^{2+}, Mn^{2+}, Co^{2+}, Cd^{2+}, Ti^{4+}, etc.; X = S^{6+}, P^{5+}, Se^{6+}, Mo^{6+}, etc.).[2−6] Langbeinite-type compounds have attracted much attention, because of their ferroelastic and ferroelectric properties,[7−11] as well as their structural phase transitions.[12−17] Recent studies have shown that, by incorporation of lanthanide ions into langbeinite-type phases, new applications may be envisaged, such as laser materials and nonlinear optical systems.[18]

Langbeinite-type phosphates, $A_xM_2(PO_4)_3$ (A = K^+, Rb^+; M = Ti^{4+}, Ti^{3+}, Yb^{3+})[19−22] form a comparably small group within the family of langbeinites, because most of these phosphates crystallize in the NASICON-type crystal structure (Sodium Super-Ionic Conductor, $Na_{1+x}Zr_2(SiO_4)_x(PO_4)_{3-x}$, space group $R\bar{3}c$).[23−28] Both the langbeinite-type and the NASICON-type structures consist of a three-dimensional framework built of corner-sharing MO_6 octahedra and PO_4 tetrahedra containing cages (for langbeinite framework) or channels (for NASICON-type structure) that are occupied by the cations.[29]

There is one very interesting alkali metal−zirconium compound in the $A_xM_2(PO_4)_3$ family, ($LiZr_2(PO_4)_3$), which is known to exhibit a complex polymorphism and a significant Li-ion conductivity.[30−33] Because of the difficulties in growing single crystals[34] and the low scattering power of Li for X-ray radiation, Catti et al. investigated the polymorphism of $LiZr_2(PO_4)_3$ via high-resolution neutron powder diffraction.[35−38] According to their work, $LiZr_2(PO_4)_3$ forms the rhombohedral NASICON-type structure (α-phase, space group $R\bar{3}c$) when prepared via solid-state reactions at 1200 °C. α-$LiZr_2(PO_4)_3$ is stable at temperatures above 60 °C and transforms to a triclinic α′-phase (space group $C\bar{1}$) during cooling. By limiting the

Received: December 7, 2010
Revised: January 28, 2011
Published: February 22, 2011

dx.doi.org/10.1021/cm103487w | *Chem. Mater.* 2011, 23, 1601–1606

synthesis temperature to 900 °C (and below), $LiZr_2(PO_4)_3$ forms an orthorhombic structure (β-phase, space group *Pbna*) and transforms to a monoclinic β'-phase (space group $P2_1/n$) at ~300 °C during cooling. The α'- and β'-phases represent distorted variants of the α- and β-phases, respectively. The solid−solid phase transitions $\alpha \leftrightarrow \alpha'$ and $\beta \leftrightarrow \beta'$ are fully reversible. Regarding the coordination and distribution of Li ions in the crystal structures, it was found that Li^+ (distributed over several sites within the lattice) shows a distorted tetrahedral coordination in the α-, α'-, and β-phase (d(Li−O) = 2.089−2.272 Å), as well as significant disorder, which can explain the significant Li-ion conductivity.[31,33,36] Only in the β'-phase (space group $P2_1/n$), Li ions are fully ordered with a regular tetrahedral coordination characterized by a smaller average distance (Li−O) of 2.024 Å that is associated with a distinctly lower Li-ion mobility.[36] Besides these phases obtained via solid-state reactions, there is also one report on the preparation of langbeinite-type (cubic) phases, "$LiZr_2(PO_4)_3$" and "$LiZr_2(PO_4)_3 \cdot 0.7H_2O$", both of which were synthesized as powders by ion-exchange reactions of cubic "$HZr_2(PO_4)_3$" in LiCl solutions.[39] However, the crystal structures of the cubic phases were not investigated in detail.

In the present work, we report on a Li-filled langbeinite variant, $Li(H_2O)_{2-x}[Zr_2(PO_4)_3]$ ($x = 0$), obtained under hydrothermal conditions. The crystal structure was determined from single-crystal X-ray data. In addition, the thermochemical properties of this compound were studied using thermogravimetry−differential thermal analysis (TG-DTA), combined with isothermal annealing experiments.

2. EXPERIMENTAL SECTION

2.1. Synthesis. $Li(H_2O)_{2-x}[Zr_2(PO_4)_3]$ ($x = 0$) was prepared under mild hydrothermal conditions. $ZrCl_4$ (0.233 g, 1 mmol, Alfa, 99.5%), $Li_2B_4O_7$ (0.324 g, 2 mmol, Sigma−Aldrich, 98%), 0.1 mL H_3PO_4 (Merck 85 wt %) and water (5.0 mL) were mixed together under constant stirring, followed by transfer to 20 mL Teflon-lined autoclaves. The pH value was adjusted to 1 via the addition of diluted HCl (ca. 10 wt %). After a reaction time of 8 days (autogenous pressure at 180 °C), the obtained products were washed with water and the solids were collected via filtration. The isolated colorless crystals with a yield of ~60 wt % (based on Zr) were first examined via powder X-ray diffraction (XRD). All reflections could be indexed by a primitive cubic cell.

2.2. Crystal Structure Determinations. The data collection for $Li(H_2O)_{2-x}[Zr_2(PO_4)_3]$ ($x = 0$) was carried out with a Rigaku AFC7 (Mercury CCD) diffractometer equipped with graphite monochromated Mo Kα radiation (λ = 0.71073 Å) at ambient temperature. A tetrahedral crystal (0.025 mm × 0.025 mm × 0.030 mm) was selected under a light microscope for single-crystal XRD analysis. Data with index ranges of $-13 \le h \le 12$, $-6 \le k \le 13$, $-12 \le l \le 13$ were collected. Based on the systematic absences, the cubic space group $P2_13$ (No. 198) was chosen. Direct methods were used to locate the Zr, P, and O atoms. The Li position was determined in the Fourier difference map. Hydrogen atoms of the crystal water molecules were not localized during the structure refinements. Direct methods implemented in the program SHELXS-97[40] were used and subsequent refinements were performed with SHELXL-97,[41] which are included in the program package WinGX.[42] A summary of the crystallographic data and refinement parameters is given in Table 1.

The powder XRD patterns of members of the series $Li(H_2O)_{2-x}[Zr_2(PO_4)_3]$ ($0 \le x \le 2$) were collected at ambient temperature on a Huber G670 diffractometer that was equipped with a graphite monochromator (Cu $K\alpha_1$ radiation, λ = 1.54060 Å). The data were collected in the 2θ range of 3°−100° with a step width of 0.005°. The lattice parameters of

Table 1. $Li(H_2O)_{2-x}[Zr_2(PO_4)_3]$ ($x = 0$): Crystallographic Data and Refinement Parameters

formula	$LiZr_2P_3O_{14}H_4$ (for $x = 0$)
space group	$P2_13$
a/Å	10.2417(1)
V/Å^3	1074.28(2)
Z	4
diffractometer	Rigaku AFC7
radiation	Mo Kα
T/K	295
2θ range/°	$5.6 \le 2\theta \le 56$
Reflect. coll.	4363
$R1$ [$I > 2\sigma(I)$]	0.047
$R1$ (all data)	0.048
$wR2$ (all data)	0.098

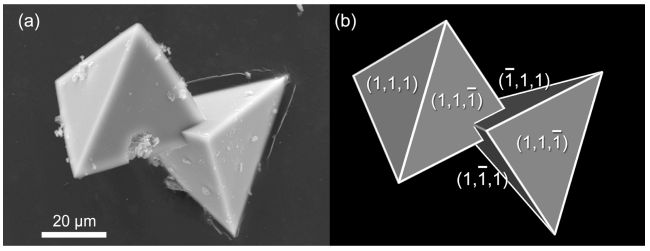

Figure 1. (a) SEM images of two intergrowth single crystals of $Li(H_2O)_{2-x}[Zr_2(PO_4)_3]$ ($x = 0$). (b) Simulation of the image shown in panel a, using a face indexing picture (produced with SHAPE by Shape Software).

$Li(H_2O)_{2-x}[Zr_2(PO_4)_3]$ ($x = 0$) were obtained from least-squares fits using 80 reflection positions extracted from the powder XRD patterns (internal standard LaB_6, NIST standard, a = 4.15692 Å at 295.5 K, WinCSD[43] program).

2.3. Thermal Analysis. Thermochemical properties of members of the series $Li(H_2O)_{2-x}[Zr_2(PO_4)_3]$ ($0 \le x \le 2$) were investigated in an argon atmosphere using simultaneous constant-rate TG-DTA up to 1200 °C (Netzsch STA 449, heating segment, 10 °C/min).

2.4. SEM-EDX. Scanning electron microscopy (SEM) images, as well as energy-dispersive X-ray spectroscopy (EDX), were carried out on three single crystals with a Philips XL 30 system with a LaB_6 cathode. With an average Zr:P molar ratio of 2.00(3):2.99(6), the obtained chemical composition agrees well with the chemical formula determined from the single-crystal structure refinements.

2.5. Chemical Analysis. The content of lithium of $Li(H_2O)_{2-x}[Zr_2(PO_4)_3]$ ($x = 0$) was confirmed by inductively coupled plasma−optical emission spectroscopy (ICP−OES) on a Varian Vista RL spectrometer with radial plasma observation. The sample was dissolved in hydrochloric acid. Li content: expt./theor. = 0.93/1.36 (w/w) (the lower experimental Li content is due to the existence of an unidentified amorphous phase in the powder sample).

3. RESULTS AND DISCUSSION

3.1. Crystal Morphology. Selected parts of the microcrystalline powder of $Li(H_2O)_{2-x}[Zr_2(PO_4)_3]$ ($x = 0$) were investigated by SEM to study the morphology. A SEM image and a simulated (indexed) model are given in Figure 1. The crystal shape is perfectly tetrahedral. Interestingly, it was reported that the parent mineral langbeinite exhibits the same morphology with edge lengths up to 15 cm.[44] The four faces of each crystal

Table 2. $Li(H_2O)_{2-x}[Zr_2(PO_4)_3]$ ($x = 0$): Fractional Coordinates and Isotropic/Equivalent Displacement Parameters (U^*_{iso}/U_{eq})

atom[a]	site	x	y	z	U^*_{iso}/U_{eq}
Zr1	4*a*	0.8603(1)	x	x	0.0152(3)*
Zr2	4*a*	0.5875(1)	x	x	0.0147(3)*
P	12*b*	0.0421(2)	0.7297(2)	0.1251(2)	0.0159(4)
O1	12*b*	0.0074(5)	0.0899(5)	0.3578(5)	0.0238(11)
O2	12*b*	0.0373(5)	0.2978(5)	0.4798(5)	0.0211(11)
O3	12*b*	0.2700(5)	0.5853(5)	0.3146(5)	0.0222(11)
O4	12*b*	0.0244(5)	0.8031(5)	0.2537(5)	0.0210(11)
O5w	4*a*	0.0699(6)	x	x	0.038(2)*
O6w	4*a*	0.2786(6)	x	x	0.038(3)*
Li	4*a*	0.171(4)	x	x	0.14(2)*

[a] Ow = oxygen atom of a water molecule.

Table 3. Selected Interatomic Distances and Angles in the Crystal Structure of $Li(H_2O)_{2-x}[Zr_2(PO_4)_3]$ ($x = 0$)

atomic bond (Å)		bond angle (°)	
Zr1−O2	2.048(5) 3×	O4[a]−Li−O1	56.91(18)
Zr1−O3	2.091(5) 3×	O4[b]−Li−O1	64.14(18)
Zr2−O1	2.071(5) 3×	O5w−Li−O6w	180.0(2)
Zr2−O4	2.077(5) 3×		
P−O1	1.528(5)		
P−O2	1.517(5)		
P−O3	1.524(5)		
P−O4	1.528(5)		
Li−O1	2.675(10) 3×		
Li−O4	2.536(6) 3×		
Li−O5w	1.79(7)		
Li−O6w	1.91(7)		

[a] $-x, y - {}^1/_2, -z + {}^1/_2$. [b] $-z + {}^1/_2, -x, y - {}^1/_2$.

represent the closed polyhedron {111}. This is consistent with the space group $P2_13$ determined by single-crystal XRD (crystal class 23).

3.2. Crystal Structure of $Li(H_2O)_{2-x}[Zr_2(PO_4)_3]$ ($x = 0$). $Li(H_2O)_{2-x}[Zr_2(PO_4)_3]$ ($x = 0$) crystallizes in space group $P2_13$ (No. 198) with four formula units per unit cell ($a = 10.2417(1)$ Å, $V = 1074.28(2)$ Å^3). Atom positions are given in Table 2, and selected interatomic distances and angles in the crystal structure of $Li(H_2O)_{2-x}[Zr_2(PO_4)_3]$ ($x = 0$) are summarized in Table 3. The crystal structure represents the langbeinite framework, which consists of ZrO_6 octahedra and PO_4 tetrahedra linked to each other by sharing all of their corners (Figure 2). There are two different crystallographic sites occupied by Zr^{4+} ions. Both are located on the 3-fold axes and are 6-fold coordinated by oxygen atoms. The Zr1 coordination octahedron is slightly distorted with Zr1−O distances of 3 × 2.048(5) Å and 3× 2.091(6) Å, whereas the Zr2−O distances are equal, within the standard deviations: 3 × 2.071(5) Å and 3 × 2.077(5) Å. P−O distances in the phosphate tetrahedra vary from 1.517(5) Å to 1.528(5) Å, with an average distance of 1.524(5) Å, which is in accordance with the expectations for nonprotonated phosphate groups.[45] The alternating ZrO_6 octahedra and PO_4 tetrahedra form ellipsoidal cages via an arrangement of six 6-membered and

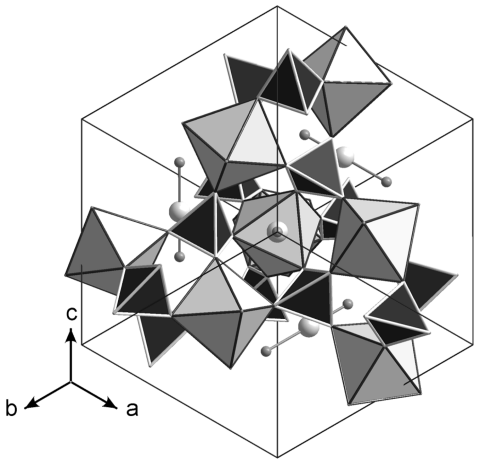

Figure 2. Crystal structure of $Li(H_2O)_{2-x}[Zr_2(PO_4)_3]$ ($x = 0$) viewed along the [111] direction. ZrO_6 octahedra (gray) and PO_4 tetrahedra (black) linked to each other by sharing common corners; Li atoms (big spheres) and O atoms of crystal water (small spheres) are situated in cages extending along the 3-fold axes. Shown is the formation of linear arrangements $H_2O\cdots Li\cdots OH_2$.

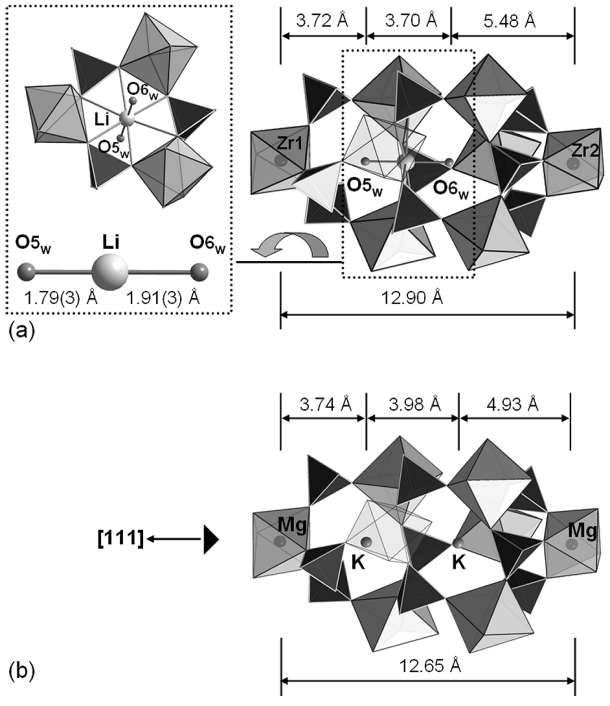

Figure 3. Comparison of the crystal structures of (a) $Li(H_2O)_{2-x}[Zr_2(PO_4)_3]$ ($x = 0$) and (b) langbeinite ($K_2Mg_2(SO_4)_3$). (a) Ellipsoidal cage formed by ZrO_6 octahedra (gray) and PO_4 tetrahedra (black) with the foremost ZrO_6 polyhedron being transparent, to enhance the visibility of the Li position. Li is surrounded by two water molecules and six O atoms from the framework. (b) Ellipsoidal cage formed by MgO_6 octahedra (gray) and SO_4 tetrahedra (black). K^+ ions take the positions of the water molecules in the phosphate.

three 4-membered rings of polyhedra (Figure 3a). The cages are filled by one Li^+ ion and two crystal water molecules. As shown in the left part of Figure 3a, an asymmetric linear coordination of Li by the two water molecules is formed, characterized by H_2O−Li distances d(Li−O5w) = 1.79(7) Å and d(Li−O6w) = 1.91(7) Å

dx.doi.org/10.1021/cm103487w |*Chem. Mater.* 2011, 23, 1601–1606

(Table 3). Six oxygen atoms of the framework complete the [2 + 6] coordination around Li (d(O−Li) = 3 × 2.536(6) Å and 3 × 2.675(10) Å; the corresponding angles for O−Li−O are 3 × 56.91(18)° and 3 × 64.14(18)°; see Table 3.

Several attempts were made to rationalize the overall crystal structure of langbeinite-type compounds,[29,46] especially with respect to the NASICON framework. The simplest approach just describes the langbeinite-type structure as a cubic rod packing of cation coordination polyhedra, whereas the NASICON structure exhibits a hexagonal arrangement. In this description, the rods in the cubic phase are aligned along the [111] direction.[47]

For comparison, the crystal structure of the mineral langbeinite, $K_2Mg_2(SO_4)_3$, is shown in Figure 3b. In the parent structure type, each cage is occupied by two K^+ ions on two crystallographically independent sites (K···K distance = 3.98 Å).[1] In the crystal structure of $Li(H_2O)_{2-x}[Zr_2(PO_4)_3]$ (x = 0), the large cages extending along the 3-fold axes were occupied by water molecules, thereby completing the langbeinite-type structural arrangement: $\{(H_2O)_2[Zr_2(PO_4)_3]\}^-$ vs $K_2[Mg_2(SO_4)_3]$. The filled langbeinite variant is completed by additional Li^+ ions by taking positions between two neighboring water molecules and via the formation of linear arrangements $H_2O\cdots Li^+\cdots OH_2$ (Figure 3a). The two positions within the cage taken by neutral water molecules ($H_2O\cdots OH_2$ distance of 3.70 Å), together with one Li ion being placed between them, is a novel situation in the structural chemistry of langbeinites and displays a rare coordination environment for Li. A similar, but symmetric, linear group was reported for $LiCl\cdot H_2O$ only recently;[48] however, the H_2O−Li distance is significantly longer (2.036(1) Å) and four Cl^- ions complete the first coordination sphere (4 × 2.630(1) Å). In the crystal structure of $Li(H_2O)_{2-x}[Zr_2(PO_4)_3]$ (x = 0), six non-Ow oxygen atoms, which are arranged to form an almost planar hexagon (Figure 3a), are the next neighbors around Li. According to the values of the Li−O distances (3 × 2.536(6) Å and 3 × 2.675(10) Å), these Li−O interactions are rather weak (8-fold coordination: sum of ionic radii of Li^+ and O^{2-} ions is calculated to be 2.34 Å[49]). Besides, it was suggested, for langbeinite-type zirconium phosphates $AZr_2(PO_4)_3$ (A = NH_4^+, H_3O^+, H^+, Na^+) obtained as powders,[39] that the monovalent ion takes both crystallographic sites with half occupation, thereby leaving a lot of space within the cage. Consequently, it was suspected[39] that additional water can be incorporated and the lattice parameters could increase as the amount of water molecules increases. This scenario can now be verified with the crystal structure determination of $Li(H_2O)_{2-x}[Zr_2(PO_4)_3]$ (x = 0). Compared to the value of a = 10.200 Å for $LiZr_2(PO_4)_3\cdot 0.7H_2O$,[39] the maximum water content in $Li(H_2O)_{2-x}[Zr_2(PO_4)_3]$ (x = 0) results in an increase of the lattice parameter to 10.2417(1) Å. A more-detailed discussion on water contents and cell parameters is given below (see also Figure 5).

3.3. Thermochemical Properties. The thermochemical properties of $Li(H_2O)_{2-x}[Zr_2(PO_4)_3]$ ($0 \le x \le 2$) were investigated via TG-DTA, accompanied by isothermal annealing. The TG curve (Figure 4) of the fully hydrated phase shows a broad weight loss (7.13 wt %) between ambient temperature and 1200 °C, which is attributed to the release of crystal water (calculated: 7.05 wt %). The corresponding DTA curve indicates that the crystal water is removed gradually, according to the two endothermic peaks with their maxima at 188 and 322 °C. After TG-DTA up to 1200 °C, the decomposition product was found to be the α′-phase (via powder XRD analysis) at ambient

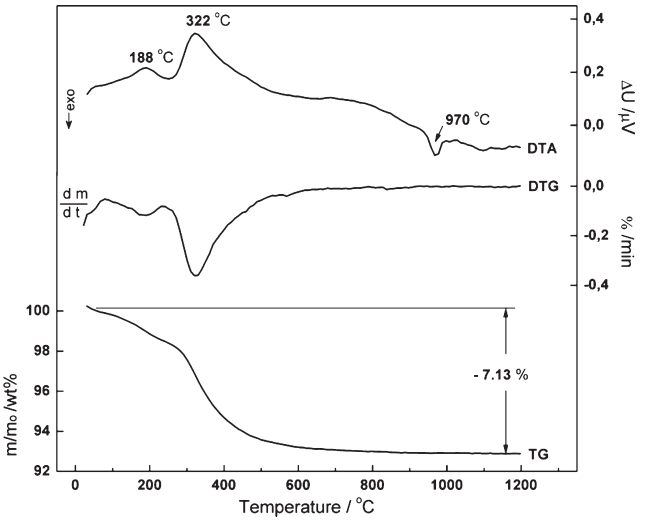

Figure 4. TG, DTG, and DTA curves of $Li(H_2O)_{2-x}[Zr_2(PO_4)_3]$ (x = 0) between ambient temperature and 1200 °C. For further details, see the text.

Table 4. Experimental Conditions of Isothermal Annealing of $Li(H_2O)_{2-x}[Zr_2(PO_4)_3]$ (x = 0) in Air and the Obtained Reaction Products Identified by Powder X-ray Diffraction at Ambient Temperature

annealing conditions	products
	$Li(H_2O)_{2-x}[Zr_2(PO_4)_3]$ (x = 0) (cubic, a = 10.2417(1) Å)
250 °C, 5 h	$Li(H_2O)_{2-x}[Zr_2(PO_4)_3]$ ($0 < x < 2$) (cubic, a = 10.1672(3) Å)
600 °C, 5 h	$Li(H_2O)_{2-x}[Zr_2(PO_4)_3]$ (x = 2) (cubic, a = 10.1565(2) Å)
800 °C, 5 h	β'-$LiZr_2(PO_4)_3$ (monoclinic)
1180 °C, 15 h	α′-$LiZr_2(PO_4)_3$ (triclinic); impurities: ZrO_2 and $Zr_2O(PO_4)_2$

temperature. To study the intermediate products during the dehydration process, further isothermal annealing experiments on $Li(H_2O)_{2-x}[Zr_2(PO_4)_3]$ (x = 0) were carried out at 250, 600, 800, and 1180 °C, respectively. The results are summarized in Table 4. Powder XRD analyses show that lattice parameter a decreases gradually with the loss of crystal water until the anhydrous cubic phase is formed (attempts to rehydrate the anhydrous cubic phase in water failed). Assuming that the lattice parameter a changes linearly (Vegard's law) with the amount of water released from members of the series $Li(H_2O)_{2-x}[Zr_2(PO_4)_3]$ ($0 \le x \le 2$), the x value for a sample treated at 250 °C for 5 h (see Table 4) is estimated to be 1.75 (see Figure 5). By taking into account the relations shown in Figure 5, the compound reported to contain $0.7H_2O$ (a = 10.200 Å)[39] would be more consistent with a monohydrate. According to the DTA curve (Figure 4), the anhydrous cubic phase is metastable and transforms exothermally at 970 °C to a stable phase (probably the known α-phase; NASICON-type structure). The feature of the irreversible release of crystal water, together with the fact that the dehydrated phase retains the cubic host structure, demonstrate that $Li(H_2O)_{2-x}[Zr_2(PO_4)_3]$ (x = 0) is a suitable precursor for the metastable dehydrated phase (x = 2). Depending on the maximum

dx.doi.org/10.1021/cm103487w |Chem. Mater. 2011, 23, 1601–1606

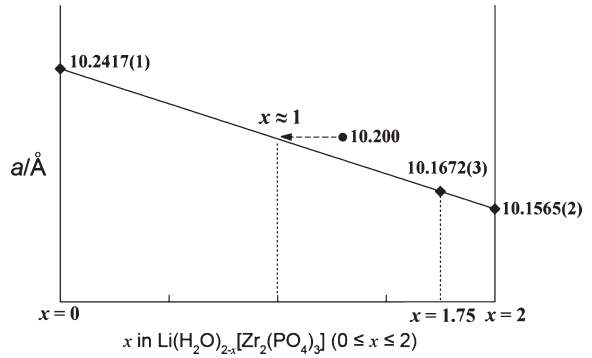

Figure 5. Assumption of a linear relationship (Vegard's law) between the lattice parameters a and the amount of released water for the series $Li(H_2O)_{2-x}[Zr_2(PO_4)_3]$ ($0 \le x \le 2$); fixed experimental values for $x = 0$ and $x = 2$. $x = 1.75$ results from the experimental a-value (see Table 4) for a sample heated at 250 °C for 5 h. $a = 10.200$ Å was reported for a compound containing $0.7H_2O$;[39] this value, however, would be more consistent with a monohydrate.

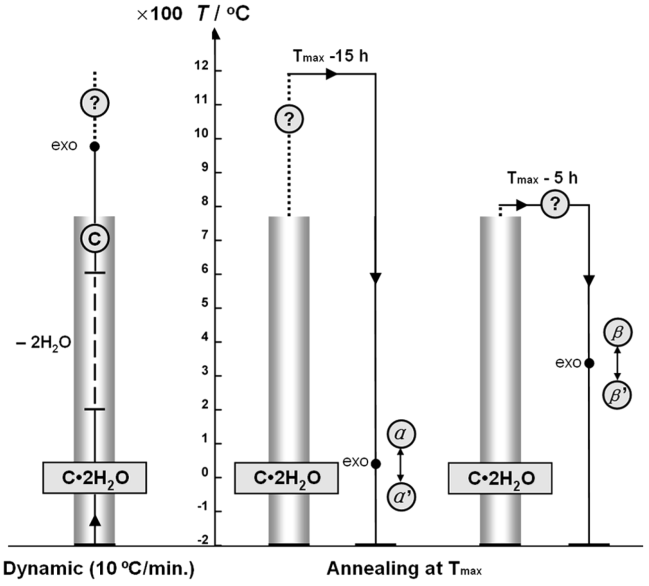

Figure 6. Summary on the thermochemical behaviors of $Li(H_2O)_{2-x}[Zr_2(PO_4)_3]$ ($x = 0$: $C \cdot 2H_2O$). TG-DTA (dynamic, left side of the T-scale) and isothermal annealing (right side of the T-scale). The release of water from the cubic hydrate and the formation of the metastable anhydrous cubic phase is presented in the gray columns. Dotted lines and question marks represent processes that have not been investigated in detail.

temperatures chosen for long-time annealing procedures (1180 and 800 °C), the rhombohedral α and orthorhombic β high-temperature phases are formed, which undergo reversible phase transitions to the triclinic α′ (~60 °C)[35] and monoclinic β' low-temperature phases (~300 °C),[36] respectively.

Langbeinite-type compounds exhibit their cubic crystal structures at ambient temperature. For some compounds, such as $Tl_2Cd_2(SO_4)_3$, however, a sequence of phase transitions is observed at low temperatures:[8,17]

$$P2_13 \xrightarrow{128\ K} P2_1 \xrightarrow{119\ K} P1 \xrightarrow{98\ K} P2_12_12_1$$

With this in mind, the title phases (hydrated, dehydrated) were investigated down to −170 °C via DTA. No indications for phase transitions at low temperatures were observed (see the Supporting Information). In addition, DTA investigations of the α′- and β'-phases were performed and the following observations were made:[34]

α′ → α solid−solid phase transition (endothermic peak during heating at 59 °C);
α → α′ solid−solid phase transition (exothermic peak during cooling at 38 °C);
β' → β solid−solid phase transition (endothermic peak during heating at 318 °C); and
β → β' solid−solid phase transition (exothermic peak during cooling at 315 °C)(See the Supporting Information.)

A summary of the thermochemical behavior of $Li(H_2O)_{2-x}[Zr_2(PO_4)_3]$ ($x = 0$) is presented in Figure 6.

4. CONCLUSIONS

A Li-filled langbeinite variant $Li(H_2O)_{2-x}[Zr_2(PO_4)_3]$ ($x = 0$) was synthesized under mild hydrothermal conditions and was structurally characterized by single-crystal X-ray diffraction. The crystal structure exhibits a langbeinite-type framework by interconnection of corner-sharing octahedra and tetrahedra, thereby forming ellipsoidal cages that are filled with asymmetric linear $H_2O-Li-OH_2$ units. Six oxygen atoms from the framework complete a [2 + 6] coordination around Li. This type of cation coordination is novel in the structural chemistry of langbeinites. The thermochemical properties of $Li(H_2O)_{2-x}[Zr_2(PO_4)_3]$ ($0 \le x \le 2$) were investigated by TG-DTA, as well as via isothermal annealing. The results reveal the formation of a dehydrated metastable cubic phase after the irreversible release of crystal water. Depending on the maximum temperatures of heat treatment, the dehydrated metastable cubic phase exothermally transforms to the known monoclinic β-phase or triclinic α-phase of $LiZr_2(PO_4)_3$, which then undergo reversible phase transitions to the low-temperature phases α′ (~60 °C) and β' (~300 °C), respectively. The dehydrated cubic phase is expected to show a high Li-ion conductivity. Because of the metastable character of this phase, a stabilization of the crystal structure is needed to prevent a monotropic phase transformation.

■ ASSOCIATED CONTENT

Supporting Information. Low temperature DTA curves of $Li(H_2O)_{2-x}[Zr_2(PO_4)_3]$ ($x = 0$), $Li(H_2O)_{2-x}[Zr_2(PO_4)_3]$ ($x = 2$), α′-$LiZr_2(PO_4)_3$ and β'-$LiZr_2(PO_4)_3$. This material is available free of charge via the Internet at http://pubs.acs.org.

■ AUTHOR INFORMATION

Corresponding Author

*Fax: +49-(0)-351-46463002. E-mail address: kniep@cpfs.mpg.de.

■ ACKNOWLEDGMENT

We thank Mrs. A. Völzke and Dr. G. Auffermann for chemical analyses, Mrs. P. Scheppan for EDX analyses, and Mrs. S. Scharsach for DTA/TG measurements. This project was supported by the "State 973" Project (No. 2007CB936704) and the Major Basic Research Programs of Shanghai (No. 07DJ14001).

■ REFERENCES

(1) Zemann, A.; Zemann, J. *Acta Crystallogr.* **1957**, *10*, 409.

(2) Kohler, V. K.; Franke, W. *Acta Crystallogr.* **1964**, *17*, 1088.
(3) Klevtsov, P. V.; Kim, V. G.; Klevtsova, R. F.; Glinskaya, L. A.; Solodovnikov, S. F. *Sov. Phys. Crystallogr.* **1988**, *33*, 30.
(4) Orlova, A. I.; Orlova, V. A.; Beskrovnyi, A. I.; Trubach, I. G.; Kurazhkovskaya, V. S. *Crystallogr. Rep.* **2005**, *50*, 759.
(5) Ogorodnyk, I. V.; Zatovsky, I. V.; Slobodyanik, N. S.; Baumer, V. N.; Shishkin, O. V. *J. Solid State Chem.* **2006**, *179*, 3461.
(6) Swain, D.; Row, T. N. G. *Acta Crystallogr. Sect. E: Struct. Rep. Online* **2006**, *62*, m138.
(7) Jona, F.; Pepinsky, R. *Phys. Rev.* **1956**, *103*, 1126.
(8) Brezina, B.; Havranko, M. *Phys. Status Solidi A* **1974**, *21*, k39.
(9) Abrahams, S. C.; Bernstein, J. L. *J. Chem. Phys.* **1977**, *67*, 2146.
(10) Lissalde, F.; Abrahams, S. C.; Bernstein, J. L.; Nassau, K. *J. Appl. Phys.* **1979**, *50*, 845.
(11) Percival, M. J. L.; Salje, E. *Phys. Chem. Miner.* **1989**, *16*, 569.
(12) Dvorak, V. *Phys. Status Solidi B* **1972**, *52*, 93.
(13) Babu, D. S.; Sastry, G. S.; Sastry, M. D.; Dalvi, A. G. I. *J. Phys. C.: Solid State Phys.* **1984**, *17*, 4245.
(14) Speer, D.; Salje, E. *Phys. Chem. Miner.* **1986**, *13*, 17.
(15) Devarajan, V.; Salje, E. *Phys. Chem. Miner.* **1986**, *13*, 25.
(16) Hikita, T.; Tanimoto, M.; Onodera, A.; Iwanaga, H. *Ferroelectrics* **1999**, *229*, 115.
(17) Guelylah, A.; Madariaga, G.; Morgenroth, W.; Aroyo, M. I.; Breczewski, T.; Bocanegra, E. H. *Acta Crystallogr., Sect. B: Struct. Sci.* **2000**, *56*, 921.
(18) Carvajal, J. J.; Aznar, A.; Sole, R.; Gavalda, J.; Massons, J.; Solans, X.; Aguilo, M.; Diaz, F. *Chem. Mater.* **2003**, *15*, 204.
(19) Masse, R.; Tordjman, I.; Durif, A.; Guitel, J. C. *Bull. Soc. Fr. Mineral. Cristallogr.* **1972**, *95*, 47.
(20) Wulff, H.; Guth, U.; Loescher, B. *Powder Diffract.* **1992**, *7*, 103.
(21) Orlova, A. I.; Trubach, I. G.; Kurazhkovskaya, V. S.; Pertierra, P.; Salvado, M. A.; Garcia-Granda, S.; Khainakov, S. A.; Garcia, J. R. *J. Solid State Chem.* **2003**, *173*, 314.
(22) Gustafsson, J. C. M.; Norberg, S. T.; Svensson, G. *Acta Crystallogr., Sect. E: Struct. Rep. Online* **2006**, *62*, i160.
(23) Sljukic, M.; Matkovic, B.; Prodic, B.; Scavnica, S. *Croat. Chem. Acta* **1967**, *39*, 145.
(24) Hagman, L. O.; Kierkega, P. *Acta Chem. Scand.* **1968**, *22*, 1822.
(25) Sljukic, M.; Matkovic, B.; Prodic, B.; Anderson, D. *Z. Kristallogr.* **1969**, *130*, 148.
(26) Alpen, U. V.; Bell, M. F.; Wichelhaus, W. *Mater. Res. Bull.* **1979**, *14*, 1317.
(27) Sugantha, M.; Varadaraju, U. V.; Rao, G. V. S. *J. Solid State Chem.* **1994**, *111*, 33.
(28) Nanjundaswamy, K. S.; Padhi, A. K.; Goodenough, J. B.; Okada, S.; Ohtsuka, H.; Arai, H.; Yamaki, J. *Solid State Ionics* **1996**, *92*, 1.
(29) Norberg, S. T. *Acta Crystallogr., Sect. B: Struct. Sci.* **2002**, *58*, 743.
(30) Casciola, M.; Costantino, U.; Merlini, L.; Andersen, I. G. K.; Andersen, E. K. *Solid State Ionics* **1988**, *26*, 229.
(31) Sudreau, F.; Petit, D.; Boilot, J. P. *J. Solid State Chem.* **1989**, *83*, 78.
(32) Nomura, K.; Ikeda, S.; Ito, K.; Einaga, H. *Solid State Ionics* **1993**, *61*, 293.
(33) Kuwano, J.; Sato, N.; Kato, M.; Takano, K. *Solid State Ionics* **1994**, *70*−*71*, 332.
(34) Petit, D.; Colomban, P.; Collin, G.; Boilot, J. P. *Mater. Res. Bull.* **1986**, *21*, 365.
(35) Catti, M.; Stramare, S.; Ibberson, R. *Solid State Ionics* **1999**, *123*, 173.
(36) Catti, M.; Morgante, N.; Ibberson, R. M. *J. Solid State Chem.* **2000**, *152*, 340.
(37) Catti, M.; Stramare, S. *Solid State Ionics* **2000**, *136*, 489.
(38) Catti, M.; Comotti, A.; Di Blas, S. *Chem. Mater.* **2003**, *15*, 1628.
(39) Ono, A.; Yajima, Y. *Bull. Chem. Soc. Jpn.* **1986**, *59*, 2761.
(40) Sheldrick, G. M. *Acta Crystallogr., Sect. A: Found. Crystallogr.* **1990**, *46*, 467.
(41) Sheldrick, G. M. *SHELXL-97—A Program for Crystal Structure Refinement*, University of Göttingen: Göttingen, Germany, 1997.
(42) Farrugia, L. J. *J. Appl. Crystallogr.* **1999**, *32*, 837.
(43) Akselrud, L. G.; Zavalii, P. Y.; Grin, Y.; Pecharski, V. K.; Baumgartner, B.; Woelfel, E. *Mater. Sci. Forum* **1993**, *133*−*136*, 335.
(44) Neitzel, U. *Kali Steinsalz* **1992**, *11*, 7.
(45) Baur, W. H. *Acta Crystallogr., Sect. B: Struct. Sci.* **1974**, *B 30*, 1195.
(46) Dross, T.; Glaum, R. *Acta Crystallogr. Sect. E: Struct. Rep. Online* **2004**, *60*, i58.
(47) Okeeffe, M; Andersson, S. *Acta Crystallogr., Sect. A: Cryst. Phys., Diffr., Theor. Gen. Crystallogr.* **1977**, *33A*, 914.
(48) Honnerscheid, A.; Nuss, J.; Muhle, C.; Jansen, M. *Z. Anorg. Allg. Chem.* **2003**, *629*, 312.
(49) Shannon, R. D. *Acta Crystallogr., Sect. A: Cryst. Phys., Diffr., Theor. Gen. Crystallogr.* **1976**, *32A*, 751.